

Journal of Materials Chemistry A

Accepted Manuscript



This is an *Accepted Manuscript*, which has been through the Royal Society of Chemistry peer review process and has been accepted for publication.

Accepted Manuscripts are published online shortly after acceptance, before technical editing, formatting and proof reading. Using this free service, authors can make their results available to the community, in citable form, before we publish the edited article. We will replace this *Accepted Manuscript* with the edited and formatted *Advance Article* as soon as it is available.

You can find more information about *Accepted Manuscripts* in the [Information for Authors](#).

Please note that technical editing may introduce minor changes to the text and/or graphics, which may alter content. The journal's standard [Terms & Conditions](#) and the [Ethical guidelines](#) still apply. In no event shall the Royal Society of Chemistry be held responsible for any errors or omissions in this *Accepted Manuscript* or any consequences arising from the use of any information it contains.

Cite this: DOI: 10.1039/c0xx00000x

www.rsc.org/xxxxxx

ARTICLE TYPE

Bioinspired Design and Assembly of Platelet Reinforced Polymer Films with Enhanced Absorption PropertiesYun-Zhao Wei, Guang-Sheng Wang*, Yun Wu, Yong-Hai Yue, Jun-Tao Wu, Chang Lu, and
5 Lin Guo**Received (in XXX, XXX) Xth XXXXXXXXX 20XX, Accepted Xth XXXXXXXXX 20XX*

DOI: 10.1039/b000000x

Bioinspired by the natural structural composites, we selectively synthesized CuS hexagonal nanoplatelets by a simple wet chemical method; and a novel approach was also developed to synthesize the brick-mortar structure CuS/PVDF nanocomposite films by self-assembly of CuS hexagonal platelets building blocks. The mechanic of the composites can increase 50 %, and the absorption peak also can reach -29.66 dB at 10.90 GHz with low filler content, the enhanced mechanism was also explained.

1. Introduction

Learning from nature is the eternal theme.^{1, 2} Natural structural composites such as teeth, bones, and seashells, have special structures and well ordered, which are the organisms to adapt to the environment, and evolved millions of years, their structures and functions have reached a perfect level. In the last decade, the novel biological inspired to design and synthesis of organic, inorganic, organic-inorganic hybrid structural materials and functional materials rapidly developed, and has become one of the hotspots in the interdisciplinary study of chemistry, materials, mechanics, life etc.^{3, 4} More recently, the microstructure of the nacre has been mimicked by several innovative techniques to fabricate the artificial nacre-like materials with high mechanical performance. For example, layer-by-layer (LBL) deposition combining with cross-linking yielded poly(vinyl alcohol)/MTM nacre-like nanocomposites with a tensile strength of up to 400 MPa; ^{5, 6} the ice-crystal templates of the microscopic layers were designed to form a brick-and-mortar microstructured Al₂O₃/poly(methylmethacrylate) composite that is 300 times tougher than its constituents; ^{7, 8} the assembly of Al₂O₃ platelets on the air/water interface and sequent spin coating was developed into the fabrication of lamellar Al₂O₃/chitosan hybrid films with high flaw tolerance and ductility; ¹ the self-assembly of nanoclays with polymers coating by a paper-making method resulted in the nacre-mimetic films; ^{9, 10} and nacre-like structural MTM-polyimide nanocomposites were fabricated by centrifugation deposition-assisted assembly.¹¹ Yu has also fabricated nacre-like chitosan-layer double hydroxide hybrid films by sequential

dipping coating and the LBL technique.¹² For the composites, too many artificial nacre-like materials with high mechanical performance have been synthesized, and the concept of mimicking nacre and recently developed innovative techniques inspired us to fabricate the highly sustainable artificial nacre-like nanocomposite film with multi-functional performance to seek a promising material for the enhanced properties of the conventional petroleum-based plastics.

On the other hand, with continuing high growth of the demands for reduction of the electromagnetic radiation and improvement of electromagnetic interference shielding, microwave-absorbing materials are widely applied in industrial, commercial and military fields.¹³⁻¹⁸ Thus, extensive studies on microwave absorption properties of various materials have been carried out for investigating microwave-absorbing materials with high and wide-band microwave absorption capacities. The most current research is focused on the electromagnetic properties in the range from 2 GHz to 18 GHz^{19, 20} For examples, Liu et al. ²¹ obtained the microwave absorbing properties of the SiC fiber/paraffin wax composite and the optimum reflection loss (RL) was -28.47 dB at 12 GHz. Meng et al.²² found that the minimum RL of the SiC microtubes was -23.9 dB at 17.5 GHz. Liu et al.²³ reported that the RL peak value of polypyrrole-reduced graphene oxide-Co₃O₄ nanocomposites was -33.5 dB at 15.8 GHz. Xu et al.²⁴ found that the smart composite absorbers mixed with silicone rubber, multi-walled carbon nanotubes and flaky carbonyl iron particles in a two-roll mixer exhibited microwave absorbing properties floated in the frequency of about 4–11 GHz. Feng et al.²⁵ reported that the flaky Ni(Fe) alloy showed microwave absorption properties of -23.8 dB at the frequency of 0.8 GHz. Many 1D nanostructures, such as carbon nanotubes,^{26,27} Fe encapsulated within carbon nanotubes,²⁸ ZnO nanostructures,²⁹⁻³¹ CdS/-Fe₂O₃ heterostructures,³² have been attracting great interests as microwave absorption materials. Some researchers have also investigated the wave absorption properties of MnO₂.^{33, 34,35} However, from the existing reports that we can find,^{36,37} most of the composites are prepared by paraffin wax, and there is still a long distance to apply in daily life. Fortunately, our recent study

shows that inorganic-organic nanocomposites, in which the paraffin wax was replaced by poly(vinylidene fluoride) (PVDF), PVDF, which is a polymer with flexible properties and can be tailored as you want.³⁸ PVDF is chosen as composite polymeric matrix materials in the fabrication of inorganic-organic nanocomposites also because of its specific physical properties and excellent dielectric properties,³⁸⁻⁴⁰ which can overcome the drawbacks of paraffin wax based composites. Besides, our research also revealed that existence of synergic effect between PVDF and nanofillers, which could distinctly enhance the wave-absorption of nanocomposite.

Copper sulfide (CuS), has been known as an important semiconductor with excellent optical, electrical, and chemical properties, and has recently attracted significant research interest for its potential applications in commercial, military and scientific electronic devices.⁴¹⁻⁴⁷ More recently, its excellent wave-absorption properties are also confirmed by our group¹³.³⁸ From the mentioned above, if we can synthesize the CuS hexagonal platelet, which is selected as a constructed unit in the layer-by-layer film, the artificial nacre-like nanocomposite film with multi-functional (increased mechanical and enhanced absorption properties) performance can be realized.

Herein, we introduce a simple wet chemical method to fabricate CuS hexagonal platelets, the growth mechanism and the reaction condition was investigated; and a novel approach was also developed to synthesize the artificial nacre-like CuS/PVDF nanocomposite films by self-assembly of CuS hexagonal platelets building blocks, the mechanic and the absorption properties were also studied in detail and the enhanced mechanism was explained.

2. Experimental

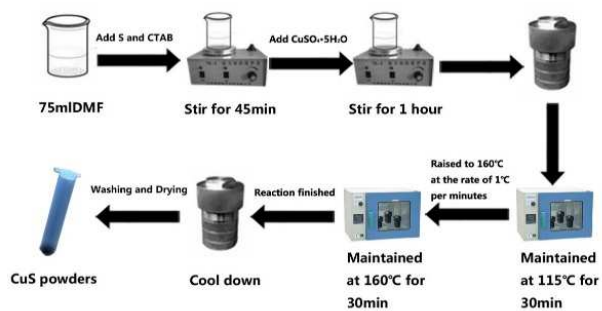


Figure 1 The synthesized process of CuS hexagonal platelets.

2.1 Preparation of CuS nanoplatelets (shown in Figure 1).

The copper sulfide nanoplatelets were synthesized by the reaction of $\text{CuSO}_4 \cdot 5\text{H}_2\text{O}$, CTAB and sulfur powder, the molar ratio of sulfur powder to $\text{CuSO}_4 \cdot 5\text{H}_2\text{O}$ was fixed. Typically, at room temperature, *N,N*-Dimethylformamide (75 ml) was used as the starting solvent. Under magnetic stirring, add a certain amount of CTAB and sulfur powder to this system, after 45 minutes, add $\text{CuSO}_4 \cdot 5\text{H}_2\text{O}$ with a certain ratio to the sulfur powder. Keep

stirring for 1 hour to create a steady solution. Transferred this solution into a Teflon-lined, stainless-steel autoclave (100 ml) and then sealed the autoclave and maintained it at 115 °C for 30 minutes to make sure the temperature of the autoclave was 115 °C. Then, the temperature rose to 160 °C at a rate of 1 °C per minute. Keep 30 minutes at the temperature of 160 °C. After reaction, the solution was cooled to room temperature, the obtained black solid products were collected by centrifuging the mixture, and then washed with absolute ethanol for three times each and then dried at 60 °C for 24 hours before further characterization.

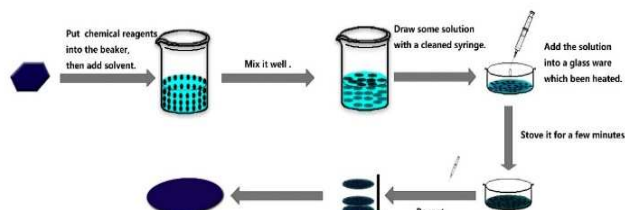


Figure 2 The synthesized process of multi-layer composite films.

Mass ratio (CuS/Total)	CuS	PVDF	DMF
5%	0.0066 g	0.1251 g	100 ml
10%	0.0139 g	0.1251 g	100 ml
15%	0.0221 g	0.1251 g	100 ml
20%	0.0313 g	0.1251 g	100 ml

Table 1 The CuS hexagonal nanoplatelets and PVDF with different ratio.

2.2 Preparation of CuS/PVDF composites.

The PVDF molecules are very easily coated onto exfoliated CuS nanoplatelets to yield the hybrid building blocks by strong electrostatic interactions. The CuS hexagonal nanoplatelet building blocks and PVDF can be dispersed in DMF with different ratio (Table 1) and then aligned to a nacre-like lamellar microstructure. For a typical process: We fabricated multi-layer composites by using an approach that relies on the natural deposition of inorganic and organic solution at ambient conditions (Figure 2), and the thickness can be controlled by calculating the volume of the solution. Because the synthesized CuS hexagonal nanoplatelet with an edge length of about 6~10 μm and a thickness of about 500 nm, most important, the density of CuS is higher than that of PVDF, the platelets will be lying and well arranged in the solution after ultrasonication for a few minutes, which was used as a means to direct their assembly into a highly oriented two-dimensional (2D) structure, after the stove process, and repeated the process mentioned above, the free-standing film formed. The fabrication process is simple, fast, time-saving, and easily scaled up compared with the LBL,⁴⁸ ice-crystal-template,⁴⁹ and other techniques.⁵⁰

2.3 Characterization.

The samples were characterized by X-ray diffraction pattern (XRD), which recorded on a (Philips X'Pert Pro Super) X-ray powder diffractometer with Cu KR radiation ($\lambda=0.154056$ nm). The grain morphology and size were observed by sputtering with gold for scanning electron microscopy (SEM) on a KYKY-1010B microscope and field-emission scanning electron microscopy (FE-SEM) on a JSM-6700F microscope. Transmission electron microscopy (TEM) and high-resolution TEM (HRTEM) investigations were carried out by a JEOLJEM-2100F microscope. Relative permittivity ϵ values were measured in the 2–18 GHz range with an Anritsu 37269D network analyzer. All the reagents (analytical-grade purity) were purchased from Beijing Chemical Reagents Co. and used without further purification.

3. Results and Discussion

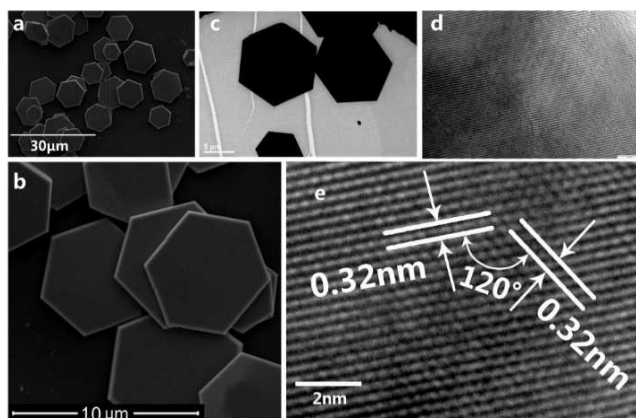


Figure 3 The SEM, TEM and HRTEM images of the typical CuS hexagonal platelets.

The SEM images in **Figure 3a, b** reveal the typical structure of the product. This product can be described as hexagonal nanoplatelet with an edge length of about 6–10 μm and a thickness of about 500 nm. The TEM and HRTEM images (**Figure 3c, d and e**) were also used to describe the morphologies and microstructures of the CuS nanomaterials. The results obtained using TEM are basically in accordance with those provided by SEM. **Figure 3e** shows the HRTEM images of the product. Through the image we learned that the lattice spacing is 0.32 nm, which is consistent with the distance between the $\{102\}$ lattice planes, thus indicating the single-crystalline nature of the CuS nanoplatelets.

The CuS hexagonal platelets were synthesized with a simple wet chemical method. The phase and purity of the as-obtained dried powder products were shown in **Figure 4**. All of the diffraction peaks of the product can be exclusively indexed to a pure hexagonal phase of CuS (JCPDS No. 06-464). No peaks for other phases were observed, thus indicating high purity and crystallinity of the products.

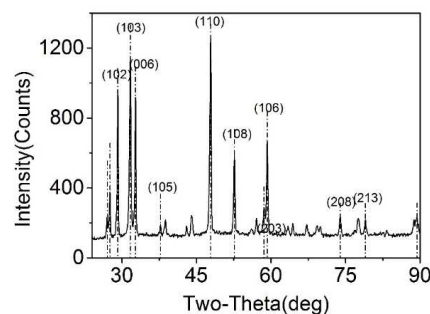


Figure 4 The XRD patterns of the synthesized product.

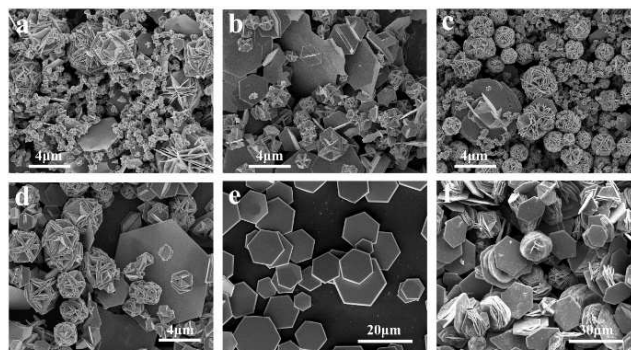


Figure 5 The SEM images of CuS product obtained using different concentration of CTAB: (a) 0.1715 mmol CTAB; (b) 0.3430 mmol CTAB; (c) 0.6860 mmol CTAB; (d) 1.3720 mmol CTAB; (e) 2.7440 mmol CTAB. (f) 5.4880 mmol.

The morphologies can be adjusted by controlling the amount of CTAB, temperature and the reaction time. By keeping the other conditions constant, the amount of CTAB in the system changed from 0.1715 mmol to 5.4880 mmol. **Figure 5a** shows that most of the products are irregular grain, some are concave polyhedron, and only a few small hexagonal nanoplatelet can be formed under this condition when the amount of CTAB increased from 0.1715 mmol to 1.3720 mmol (**Figure 5a-d**); when the amount of CTAB reached 2.7440 mmol, the irregular particles and complex concave polyhedron disappeared, replaced by hexagonal platelets, and the edge length of about 6–10 μm and a thickness of about 500 nm (**Figure 5e**). When the amount of CTAB increases to 5.880 mmol, the hexagonal platelets changed to flower-like structures (**Figure 5f**). So the direction of the CuS crystal growth can be controlled by the addition of CTAB, it indicates that the amount of CTAB in the reaction play a key action in the reaction process.

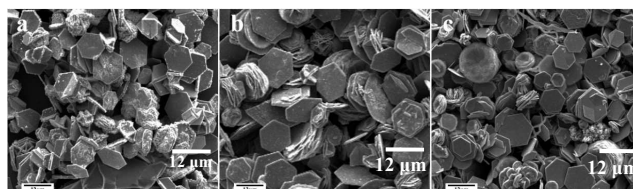


Figure 6 The SEM images of CuS product obtained using different molar ratio of S: CuSO₄: (a) 1:1; (b) 2:1; (c) 4:1.

In this reaction, the R_S (the molar ratio of S/CuSO₄·5H₂O) is also an important factor that influences the structure of the prepared product (Figure 6). When R_S is 1:1, we can find many structures such as: Vertical cross plates, hexagonal platelets and some flowers-like structures (Figure 6a). However, when the molar ratio changed to 2:1, the amount of vertical cross plates decreased, and most of the products are hexagonal nanoplatelets and a few flower-like structures (Figure 6b). When the molar ratio increased to 4:1, the amount of hexagonal platelets increased and there were still some flower-like structures in the products (Figure 6c). From mentioned above, the R_S also plays an important role in the reaction system.

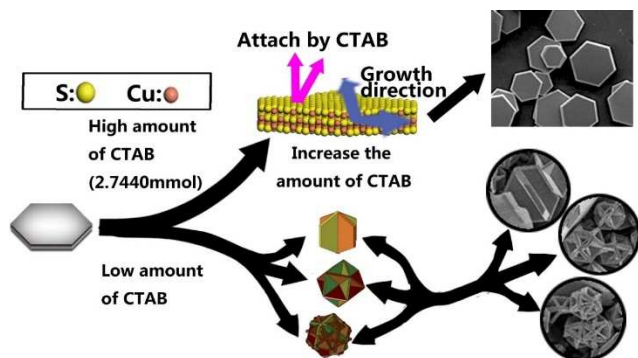


Figure 7 The growth mechanism of CuS hexagonal platelets.

Based on the previous report and the results mentioned above, we conclude that the CuS hexagonal nanoplatelet owns a highly anisotropic crystal structure, which consists of stacked CuS₄-CuS₃-CuS₄ layers and is predisposed to anisotropic growth under appropriate conditions (Figure 7). The larger-area (0001) crystal surfaces limit the exposure of other higher-energy surfaces, reducing the total energy of the nanocrystals and resulting in the formation of the stable nanoplates as observed through the TEM experiments. On the basis of the crystal structure and the above mentioned characterization results, it is believed that the crystal nuclei that grow slowly on the (1010) and (1120) planes was hindered by the high concentration of CTAB.⁵¹

In the composites, the mechanic of the CuS hexagonal platelets is an important factor. In situ Nano indentation test has been conducted in a SEM (shown in Figure S1) to measure the mechanic of the CuS hexagonal platelets, as shown in the top-left insert in Figure S1, the AFM cantilever-piezo position along the z-direction curve for a CuS nanochip under an applied bending force of about 2N has also been shown in Figure S1 as well as the SEM image of the nanochip after the nano indentation test (lower-right insert image). As we can see, the applied force and deflection keeps a good linear relationship up to 2 N. Hardness values of these nanochips are around the value of 1.3 GPa.

To investigate the inside structure of the composites affected by the concentration of CuS hexagonal platelets, various contents of CuS powders were mixed with PVDF in DMF to form CuS+PVDF solution and fabricate the films. The SEM images of composites in Figure 8a, b and c indicate excellent well oriented

dispersion of CuS hexagonal platelets and compact structure in the polymer. The CuS hexagonal platelets are still kept in the composites after the fabrication process and the space among the CuS hexagonal platelets decreases with the increasing of the weight ratio of CuS. The results of XRD (Figure 8d), in which that only (006) and (008) peak diffractions were observed in the nanocomposite. There is the direct evidence confirming that the CuS hexagonal platelets are aligned horizontally in the polymer. The FESEM characterization and elemental maps of CuS/PVDF are also displayed in Figure 8e. The elemental maps of Cu, S and C, which are on the surface of the CuS/PVDF nanocomposites also confirm the good dispersion of the CuS hexagonal platelets in PVDF. The elemental map of single platelet in the PVDF was also given in the Figure 8f, which further confirmed the good adhesion between inorganic platelets and the organic matrix (marked by a green arrow in Figure 8f). The good dispersion of the CuS hexagonal platelets in PVDF may be helpful for the dielectric and absorption properties. In addition, from the photograph of the CuS/PVDF film in Figure S2, this film also exhibits excellent flexibility. The relation between the electrical conductivity and the filler content was also studied shown in Table S1, and the electrical conductivity increased with the increasing filler content.

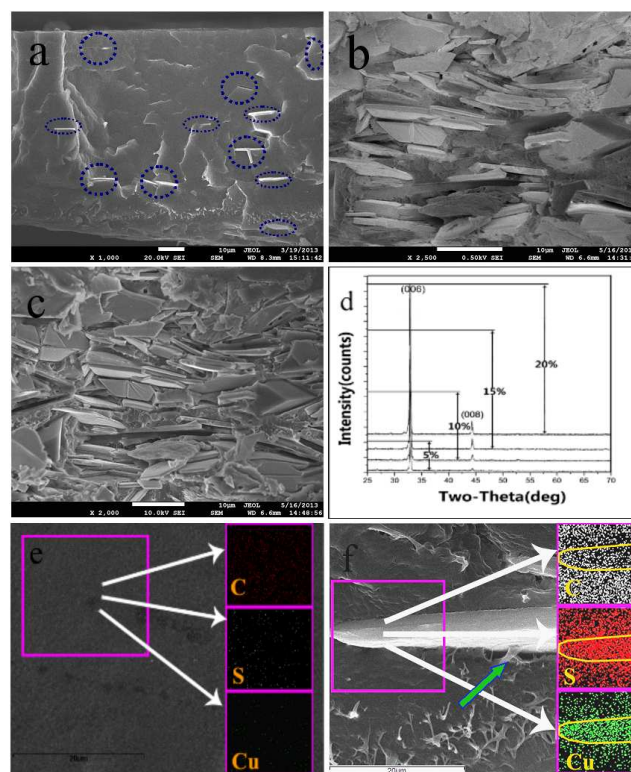


Figure 8 A cross-sectional SEM image of the composite with the different weight ratio: (a) 0.10; (b) 0.15; (c) 0.20; (d) the samples over self-assembly were determined from the XRD patterns; (e, f) FESEM image of the CuS/PVDF composites and corresponding elemental mapping images of Cu, S and C.

Flexible and thin hybrid films with different loading from 5 wt% to 20 wt% exhibited a brick-mortar structure with strongly

aligned platelets surrounded by a ductile organic matrix (**Figure 9**), we conclude that the structure can enhance tensile properties.¹ To confirm the hypothesis, the tensile properties of the pure PVDF, composites filled with CuS hexagonal platelets have been tested, the PVDF filled with the loading 10 wt% CuS hexagonal platelets without the brick-mortar structure was also given in **Figure S3**. The results (shown in Table 2, which is the Max tensile strain with different loading content) indicate that the tensile strength of the composite with different loadings show higher tensile strain than that of the pure PVDF (27.83 MPa), and increased with the increasing loading, when the loading is higher than 15 wt%, the tensile strength decreased. Typically, both the composites with loading 10 wt% and 15 wt%, the tensile strength is 1.5 times higher than that of the pure PVDF. And with the same loading 10 wt%, the tensile strength with brick-mortar structure is obviously higher than that of the irregular composites (about 30.66 MPa, **Figure S3**). The composites with increased tensile properties would satisfy the need in practical applications.

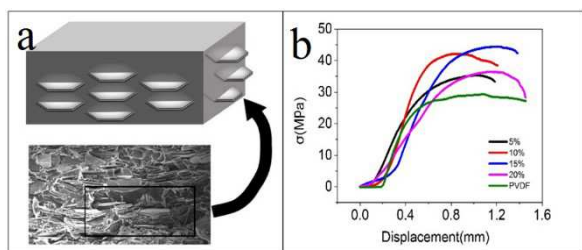


Figure 9 (a) The model of the inside brick-mortar structure; (b) the Tensile strength of the composites with different loading content.

Content of CuS	0%	5%	10%	15%	20%
The Max tensile strain (MPa)	27.83	35.35	42.13	42.47	36.44

Table 2 The table is the Max tensile strain with different loading content.

To investigate how the layer-by-layer oriented structure of CuS hexagonal platelets nanostructure affect the absorbing properties of composites, various contents of CuS powders were mixed with PVDF to form composites by the method mentioned above, and tailored the film into rings ($\Phi_{\text{out}} = 7.00$ mm and $\Phi_{\text{in}} = 3.04$ mm) and pressing the mixture into a cylindrical shaped compacted with a simple hot press method. The frequency dependence relative permittivity for several materials was investigated and shown in **Figure 10**. The real permittivities of CuS/PVDF increase with the increasing loading content **Figure 10a**, which is higher than that of pure PVDF (about 3.0). And the imaginary permittivities of CuS/PVDF (**Figure 10b**) are also higher than that of pure PVDF. It indicated that the introduction of CuS hexagonal platelets into PVDF can greatly enhance the dielectric constant of the PVDF composite, which is the same with the CuS complex nanostructures; the enhanced permittivities can be ascribed to the synergistic effect, which has been reported in previous report.^{38, 40}

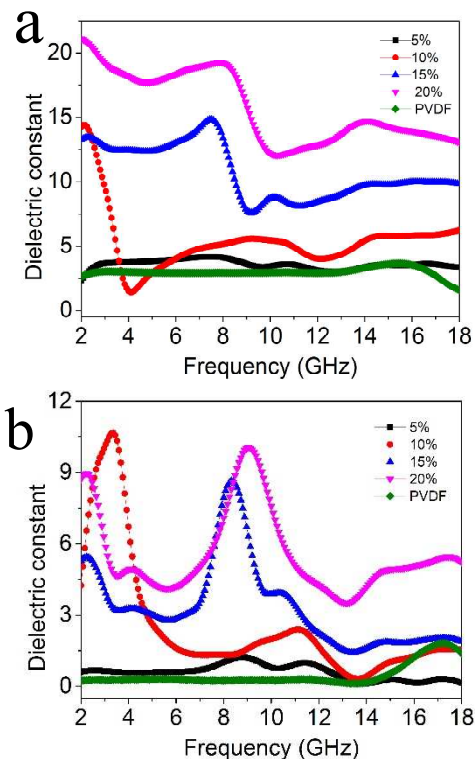


Figure 10 Measured frequency dependence of (a) real parts; (b) imaginary parts of dielectric permittivity.

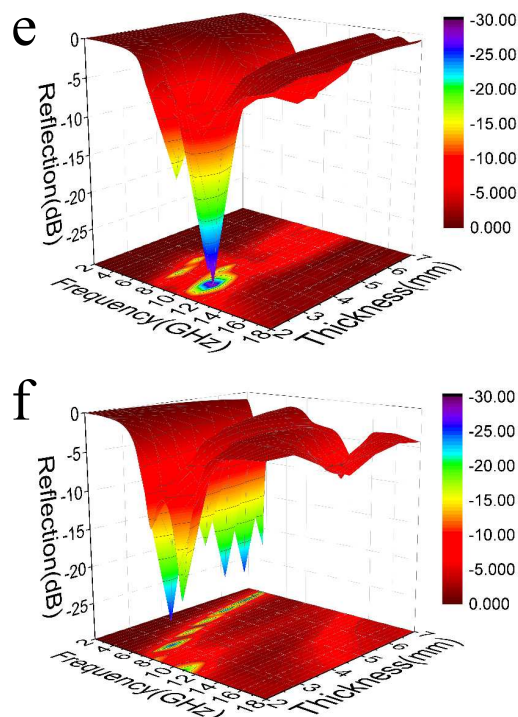
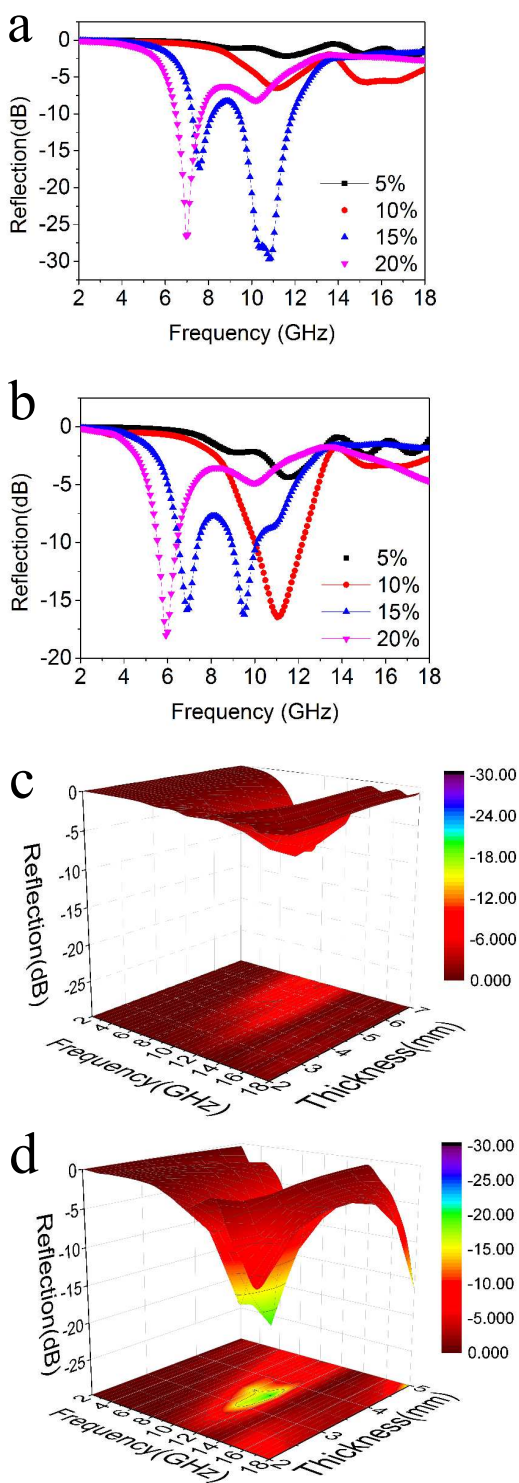
We calculated the dielectric loss tangent of CuS/PVDF composites with different loadings (as showed in **Figure S4**). All the dielectric losses of the samples are higher than that of pure PVDF at the considered frequency. Therefore, the increasing loading of CuS results in an enhancement of the dielectric loss. But the nanocomposite with loading 10 wt% of synthesized CuS hexagonal platelets increase rapidly and shows a stronger dielectric loss at about 4 GHz.

To study the microwave absorption, the reflection loss (RLs) of the electromagnetic radiation under the normal incidence of the electromagnetic field was calculated. The normalized input impedance (Z_{in}) is given by:⁵²

$$Z_{\text{in}} = \sqrt{\frac{\mu_r}{\epsilon_r}} \tanh \left[j \left(\frac{2f\pi d}{c} \right) \sqrt{\mu_r \epsilon_r} \right] \quad (1)$$

Where, ϵ_r and μ_r (for CuS hexagonal platelet, μ_r is thought as 1), are the complex permittivity and permeability of the composite absorber, respectively; f is the frequency; d is the thickness of the absorber, and c is the velocity of light in free space. The reflection loss (R) is related to Z_{in} as:⁵³

$$R = 20 \log \left| \frac{Z_{\text{in}} - 1}{Z_{\text{in}} + 1} \right| \quad (2)$$



5

Figure 11 Microwave RL curves of the composites with a thickness of 2.5 mm (a) and 3.0 mm (b) in the frequency range of 2-18 GHz; Three-dimensional presentations of RL of CuS/PVDF composites with loading 5 wt% (c); 10 wt% (d); 15 wt%(e) and 20 wt% (f).

Thus, the theoretical RL of the composite absorbers with filler loading of 5 wt%, 10 wt%, 15 wt% and 20 wt% at various thicknesses can be obtained through Eqs. (1) and (2) (shown in **Figure 11a, b**). **Figure 11a** shows the calculated theoretical RLs of the CuS/PVDF composites with different loading content under the same thickness (2.5 mm) in the range of 2–18 GHz. It can be observed that the loading content of the absorbers have a great influence on the microwave absorbing properties and the minimum RLs corresponding to the maximum absorptions gradually appeared in different frequency shift toward the lower frequency. For the composite with loading content 10 wt%, when the absorbers with a thickness of 2.5 mm, the minimum RL is obviously lower than that of the composites without the brick-mortar structure (shown in **Figure S5**), while, for the composites with loading content 15 wt%, when the absorbers with a thickness of 2.5 mm, the minimum RL and the f_m are -29.66 dB and 10.90 GHz. As mentioned above, we concluded that the as prepared CuS/PVDF composite shows the excellent absorption performances and the minimum RL can be adjusted to the different frequency by controlling the loading content, as far as we know, this phenomena is not reported by other groups. We think that the minimum RL can be adjusted to the different frequency by controlling the loading content is due to the increasing CuS hexagonal platelets in the unit area, which is another method to increase the thickness of the composites. **Figure 11b** shows the wave absorption abilities of different material at a thickness of 3 mm. We could also clearly see the

minimum RL of CuS/PVDF composite shift to the low frequency with the increasing loading content. Therefore, the enhanced wave absorption abilities can be ascribed to the synergetic effect between CuS and PVDF. We also found a higher concentration of CuS in this composite material lead to contrary microwave absorption properties: the Cu/PVDF composite with a loading of 15 wt% have a strong peak (-29.66 dB at 10.90 GHz) while the composite with a loading of 20 wt% only have a peak at frequency of 6.98 GHz (-26.56 dB). The three-dimensional presentations of RL (**Figure 11c, d, e and f**) show the calculated theoretical RLs of the CuS/PVDF composites with different thickness (2-5 mm) in the range of 2-18 GHz with the loading of 5 wt%, 10 wt%, 15 wt% and 20 wt%, respectively. It indicates that the microwave absorbing properties and the minimum RLs corresponding to the maximum absorptions gradually appeared in different frequency can be tunable by controlling the thickness of the absorbers. While, the maximum absorptions increased with the increasing loading content from 0 to 15 wt%, and then decreased. For the CuS/PVDF composites with the loading of 15 wt% shown in **Figure 11e**, there is a stronger peak (-29.66 dB at 10.9 GHz), when the absorbers with a thickness of 2.5 mm, and the stronger peak can also be adjusted by the thickness. The related physical mechanism is still not very clear so far. But based on some previous reports about the dielectric constant at low frequency, the enhancement in the dielectric constant can be explained according to the percolation theory, that is, the percolation threshold of the two-phase random composite should be about $f_c = 0.16$ if the conducting fillers are sphere particles.⁵⁴

In our composites, CuS hexagonal is well dispersed and not connected with each other in the PVDF; while, with the increasing loading content, some dispersed CuS hexagonal platelets connected the adjacent layers, that is, it reaches the percolation threshold, the conductive network makes the composite become the conducting material at different layers, and this leads to a high leakage current, which may cause damage to the wave-absorption of materials. The impedance match of this composite is also a very important characteristic for microwave absorption of material, apart from dielectric loss and magnetic loss. impedance match is another very important characteristic for microwave absorption of material, apart from dielectric loss and magnetic loss. Higher concentration of CuS may result in higher conductivity, and bring into high permittivity. Sometimes high permittivity of absorber is harmful to the impedance match and may result in weak absorption.⁵⁵ Besides, high concentration of CuS hexagonal in this composite with LBL structure also result in the occurrence of a significant skin effect as its surface is irradiated by microwave,^{56,57} for the composites with the LBL structure, skin effect maybe even worse, which cause damage to the wave-absorption of materials.

For dielectric loss material to absorb microwave, Debye dipolar relaxation is an important mechanism. And the relative complex permittivity can be expressed by the following equation,⁵⁸

$$\varepsilon_r = \varepsilon_\infty + \frac{\varepsilon_s - \varepsilon_\infty}{1 + j2\pi f\tau} = \varepsilon' - j\varepsilon'' \quad (3)$$

where f , ε_s , ε_∞ , and τ are frequency, static permittivity, relative dielectric permittivity at the high-frequency limit, and polarization relaxation time, respectively. Thus, ε' and ε'' can be described by

$$\varepsilon' = \varepsilon_\infty + \frac{\varepsilon_s - \varepsilon_\infty}{1 + (2\pi f)^2 \tau^2} \quad (4)$$

$$\varepsilon'' = \frac{2\pi f\tau(\varepsilon_s - \varepsilon_\infty)}{1 + (2\pi f)^2 \tau^2} \quad (5)$$

According to eqn (4) and (5), the relationship between ε' and ε'' can be deduced,

$$\left(\varepsilon' - \frac{\varepsilon_s + \varepsilon_\infty}{2}\right)^2 + (\varepsilon'')^2 = \left(\frac{\varepsilon_s - \varepsilon_\infty}{2}\right)^2 \quad (6)$$

Thus, the plot of ε' versus ε'' would be a single semicircle, generally denoted as the Cole–Cole semicircle. Each semicircle corresponds to one Debye relaxation process. **Figure S6** shows the ε' - ε'' curve of the loading of 5 wt%, 10 wt%, 15 wt% and 20 wt%, respectively. The ε' - ε'' plot of composites exhibits a succession of semicircles, which can be ascribed to relaxation phenomena with different time constants due to the contribution of grain (bulk), grain boundary and interface/electrode polarization. For our previous report, there is an obvious Cole–Cole semicircle in the ε' - ε'' curve of pure PVDF and an inconspicuous semicircle in CuS/Paraffin, indicating the existence of Debye relaxation process in the pure PVDF and CuS materials. However, three semicircles were clearly found in the curve of CuS/PVDF composite, representing the contribution of Debye relaxation process of CuS, PVDF and the interface of CuS and PVDF. And some slight differences of the ε' - ε'' with different loading curves exist; we think that several semicircles in each curve implied that other kinds of relaxation in CuS/PVDF system, such as Maxwell-Wagner relaxation and electron polarization. For our composites, the existence of interfaces at one oriented direction has a greatly influence on interfacial polarization or Maxwell-Wagner effect.⁵⁹⁻⁶¹ On the other hand, electron polarization also contributes to the synergistic effect. CuS hexagonal platelet is a semiconductor, which can increase conductivity of the composites. Therefore, high concentration of CuS hexagonal platelets at one orientation with lay-by-layer in this composite will increase in the conductivity of the composite.

According to the free-electron theory $\varepsilon'' \propto \sigma / 2\pi\epsilon_0 f$ (σ is the electrical conductivity), increased conductivity of composite could result in strong dielectric loss.

Conclusion

In this paper, the hexagonal platelets CuS have been selectively synthesized by a simple wet-chemical method. The brick-mortar structure CuS/PVDF nanocomposite films were fabricated with a novel approach for microwave absorption application. The inside structure was investigated in detail, which is the similar with the brick-mortar structure. Different CuS hexagonal platelets loading in the composite was studied to optimize its mechanic properties and microwave absorption properties. The mechanic of the composites can increase 50 %, and the absorption properties also reach -29.66 dB at 10.90 GHz, the enhanced mechanism was also explained. The CuS/PVDF composites possess excellent microwave absorption performance is promising to apply in commercial, military and scientific electronic devices, and the method is also suitable for industrial production.

Acknowledgement: This project was financially supported by the National Basic Research Program of China (2010CB934700) and the National Natural Science Foundation of China (Nos. 51102223, 50725208 and 51132002).

^a Key Laboratory of Bio-Inspired Smart Interfacial Science and Technology of Ministry of Education, School of Chemistry and Environment, Beihang University, Beijing 100191, PR China. wanggsh@buaa.edu.cn and guolin@buaa.edu.cn
guolin@buaa.edu.cn and guolin@buaa.edu.cn

† Electronic Supplementary Information (ESI) available: [details of any supplementary information available should be included here]. See DOI: 10.1039/b000000x/

‡ Footnotes should appear here. These might include comments relevant to but not central to the matter under discussion, limited experimental and spectral data, and crystallographic data.

Notes and references

- L. J. Bonderer, A. R. Studart and L. J. Gauckler, *Science*, 2008, **319**, 1069-1073.
- P. Fratzl, *Science*, 2012, **335**, 177-178.
- H.-B. Yao, H.-Y. Fang, X.-H. Wang and S.-H. Yu, *Chemical Society Reviews*, 2011, **40**, 3764-3785.
- H.-B. Yao, Z.-H. Tan, H.-Y. Fang and S.-H. Yu, *Angewandte Chemie International Edition*, 2010, **49**, 10127-10131.
- P. Podsiadlo, A. K. Kaushik, E. M. Arruda, A. M. Waas, B. S. Shim, J. Xu, H. Nandivada, B. G. Pumplun, J. Lahann, A. Ramamoorthy and N. A. Kotov, *Science*, 2007, **318**, 80-83.
- Z. Tang, N. A. Kotov, S. Magonov and B. Ozturk, *Nat Mater*, 2003, **2**, 413-418.
- S. Deville, E. Saiz, R. K. Nalla and A. P. Tomsia, *Science*, 2006, **311**, 515-518.
- E. Munch, M. E. Launey, D. H. Alsem, E. Saiz, A. P. Tomsia and R. O. Ritchie, *Science*, 2008, **322**, 1516-1520.
- A. Walther, I. Bjurhager, J.-M. Malho, J. Pere, J. Ruokolainen, L. A. Berglund and O. Ikkala, *Nano Letters*, 2010, **10**, 2742-2748.
- A. Walther, I. Bjurhager, J.-M. Malho, J. Ruokolainen, L. Berglund and O. Ikkala, *Angewandte Chemie*, 2010, **122**, 6593-6599.
- R. Chen, C.-a. Wang, Y. Huang and H. Le, *Materials Science and Engineering: C*, 2008, **28**, 218-222.
- J. F. Lutz, M. Ouchi, D. R. Liu and M. Sawamoto, *Science*, 2013, **341**, 1238149.
- S. He, G.-S. Wang, C. Lu, X. Luo, B. Wen, L. Guo and M.-S. Cao, *Chempluschem*, 2013, **78**, 250-258.
- J.-J. Fang, S.-F. Li, W.-K. Zha, H.-Y. Cong, J.-F. Chen and Z.-Z. Chen, *Journal Of Inorganic Materials*, 2011, **26**, 467-471.
- R. K. Srivastava, T. N. Narayanan, A. P. R. Mary, M. R. Anantharaman, A. Srivastava, R. Vajtai and P. M. Ajayan, *Applied Physics Letters*, 2011, **99**, 113116.
- A. Tadjarodi, R. Rahimi, M. Imani, H. Kerdari and M. Rabbani, *J Alloy Compd*, 2012, **542**, 43-50.
- C. Wang, X. Han, P. Xu, X. Zhang, Y. Du, S. Hu, J. Wang and X. Wang, *Appl Phys Lett*, 2011, **98**, 072906.
- G. Sun, B. Dong, M. Cao, B. Wei and C. Hu, *Chemistry Of Materials*, 2011, **23**, 1587-1593.
- W. Zhou, X. Hu, X. Bai, S. Zhou, C. Sun, J. Yan and P. Chen, *ACS Applied Materials & Interfaces*, 2011, **3**, 3839-3845.
- P. Liu, Y. Huang, L. Wang and W. Zhang, *Journal of Alloys and Compounds*, 2013, **573**, 151-156.
- X. G. Liu, Y. D. Wang, L. Wang, J. G. Xue and X. Y. Lan, *Journal Of Inorganic Materials*, 2010, **25**, 441-444.
- S. Meng, X. Y. Guo, G. Q. Jin, Y. Y. Wang and S. Xie, *Journal of Materials Science*, 2012, **47**, 2899-2902.
- P. B. Liu, Y. Huang, L. Wang and W. Zhang, *Journal of Alloys and Compounds*, 2013, **573**, 151-156.
- Y. G. Xu, L. M. Yuan, J. Cai and D. Y. Zhang, *Journal of Magnetism and Magnetic Materials*, 2013, **343**, 239-244.
- J. Liu, Y. B. Feng and T. Qiu, *Journal Of Magnetism and Magnetic Materials*, 2011, **323**, 3071-3076.
- L. M. Yu, B. Li, L. M. Sheng, K. An and X. L. Zhao, *Journal of Alloys and Compounds*, 2013, **575**, 123-127.
- Q. S. Xiao, B. Hao, L. C. Li, M. Y. Mao, Y. Zhou and F. Xu, in *Advances in Materials and Materials Processing, Pts 1-3*, eds. Z. Y. Jiang, X. H. Liu, S. H. Jiao and J. T. Han, 2013, pp. 327-330.
- R. C. Che, L. M. Peng, X. F. Duan, Q. Chen and X. L. Liang, *Advanced Materials*, 2004, **16**, 401-405.
- X.-Y. Fang, M.-S. Cao, X.-L. Shi, Z.-L. Hou, W.-L. Song and J. Yuan, *Journal Of Applied Physics*, 2010, **107**.
- M.-S. Cao, X.-L. Shi, X.-Y. Fang, H.-B. Jin, Z.-L. Hou, W. Zhou and Y.-J. Chen, *Applied Physics Letters*, 2007, **91**.
- Q. Hu, G. X. Tong, W. H. Wu, F. T. Liu, H. S. Qian and D. Y. Hong, *Crystengcomm*, 2013, **15**, 1314-1323.
- L. Wang, H. W. Wei, Y. J. Fan, X. Gu and J. H. Zhan, *Journal of Physical Chemistry C*, 2009, **113**, 14119-14125.
- G. S. Wang, L. Z. Nie and S. H. Yu, *RSC Advances*, 2012, **2**, 6216-6221.
- H. Guan, G. Chen, S. Zhang and Y. Wang, *Materials Chemistry and Physics*, 2010, **124**, 639-645.
- J. L. Deng and K. Huang, in *Advanced Engineering Materials II, Pts 1-3*, eds. C. X. Cui, Y. L. Li and Z. H. Yuan, 2012, pp. 201-205.
- M. Zhou, X. Zhang, J. Wei, S. Zhao, L. Wang and B. Feng, *Journal Of Physical Chemistry C*, 2011, **115**, 1398-1402.
- H. T. Guan, G. Chen, J. Zhu and Y. D. Wang, *Functional Materials Letters*, 2012, **5**.
- S. He, G.-S. Wang, C. Lu, J. Liu, B. Wen, H. Liu, L. Guo and M.-S. Cao, *Journal of Materials Chemistry A*, 2013, **1**, 4685-4692.
- G. Wang, *ACS Applied Materials & Interfaces*, 2010, **2**, 1290-1293.
- G.-S. Wang, X.-J. Zhang, Y.-Z. Wei, S. He, L. Guo and M.-S. Cao, *Journal of Materials Chemistry A*, 2013, **1**, 7031-7036.
- K. D. Yuan, J. J. Wu, M. L. Liu, L. L. Zhang, F. F. Xu, L. D. Chen and F. Q. Huang, *Applied Physics Letters*, 2008, **93**, 132106.
- X. L. Yu, C. B. Cao, H. S. Zhu, Q. S. Li, C. L. Liu and Q. H. Gong, *Advanced Functional Materials*, 2007, **17**, 1397-1401.
- Y. Han, Y. Wang, W. Gao, Y. Wang, L. Jiao, H. Yuan and S. Liu, *Powder Technology*, 2011, **212**, 64-68.
- X. Bo, J. Bai, L. Wang and L. Guo, *Talanta*, 2010, **81**, 339-345.
- Q. Tian, M. Tang, Y. Sun, R. Zou, Z. Chen, M. Zhu, S. Yang, J. Wang, J. Wang and J. Hu, *Advanced Materials*, 2011, **23**, 3542-3547.
- M. Basu, A. K. Sinha, M. Pradhan, S. Sarkar, Y. Negishi, Govind and T. Pal, *ENVIRONMENTAL SCIENCE & TECHNOLOGY*, 2010, **44**, 6313-6318.
- L. Reijnen, B. Meester, F. de Lange, J. Schoonman and A. Goossens, *Chemistry of Materials*, 2005, **17**, 2724-2728.
- S. Srivastava and N. A. Kotov, *Accounts of Chemical Research*, 2008, **41**, 1831-1841.
- C. A. L. Colard, R. A. Cave, N. Grossiord, J. A. Covington and S. A. F. Bon, *Advanced Materials*, 2009, **21**, 2894+.
- P. T. Hammond, *Advanced Materials*, 2004, **16**, 1271-1293.
- W. Du, X. Qian, X. Ma, Q. Gong, H. Cao and J. Yin, *Chemistry – A European Journal*, 2007, **13**, 3241-3247.
- G.-S. Wang, L.-Z. Nie and S.-H. Yu, *RSC Advances*, 2012, **2**, 6216-6221.
- X. Qi, Y. Yang, W. Zhong, Y. Deng, C. Au and Y. Du, *Journal of Solid State Chemistry*, 2009, **182**, 2691-2697.
- G. Wang, Y. Deng, Y. Xiang and L. Guo, *Advanced Functional Materials*, 2008, **18**, 2584-2592.
- C. Wang, X. Han, P. Xu, X. Zhang, Y. Du, S. Hu, J. Wang and X. Wang, *Applied Physics Letters*, 2011, **98**, 072906-072906-072903.
- G. He, H. Chen, J. Zhu, F. Bei, X. Sun and X. Wang, *Journal of Materials Chemistry*, 2011, **21**, 14631-14638.
- W.-L. Song, M.-S. Cao, M.-M. Lu, J. Liu, J. Yuan and L.-Z. Fan, *Journal of Materials Chemistry C*, 2013, **1**, 1846-1854.
- S. Stankovich, D. A. Dikin, R. D. Piner, K. A. Kohlhaas, A. Kleinhammes, Y. Jia, Y. Wu, S. T. Nguyen and R. S. Ruoff, *Carbon*, 2007, **45**, 1558-1565.
- J. K. Nelson and J. C. Fothergill, *Nanotechnology*, 2004, **15**, 586-595.
- N. Ortega, A. Kumar, R. S. Katiyar and C. Rinaldi, *Journal Of Materials Science*, 2009, **44**, 5127-5142.

61. P. K. Mandal, A. Lapanik, R. Wipf, B. Stuehn and W. Haase, *Applied Physics Letters*, 2012, **100**.

Graphic Abstract:

Bioinspired by the natural structural composites, we selectively synthesized CuS hexagonal nanoplatelets by a simple wet chemical method; A novel approach was also developed to synthesize the brick-mortar structure CuS/PVDF nanocomposite films; The mechanic of the composites can increase 50 %, and the absorption properties also reach -29.66 dB at 10.90 GHz, the enhanced mechanism was also explained.

